

# Coupling Peridynamic Simulations with Data-Driven Approaches for Intelligent Fracture Prediction in Structures

H. N. Yakin<sup>1\*</sup>, N. A. Hashim<sup>2</sup>, F. Fisol<sup>1</sup>, M. N. Mastor<sup>1</sup> and Q. Halim<sup>3</sup>

<sup>1</sup>Department of Structure & Materials, Faculty of Civil Engineering, Universiti Teknologi Malaysia, Johor, Malaysia.

<sup>2</sup>Faculty of Civil Engineering & Technology, Universiti Malaysia Perlis (UniMAP), Kompleks Pusat Pengajian Jejawi 3, Arau, Perlis, Malaysia.

<sup>3</sup>MRANTI Corporation Sdn. Bhd., Technology Park Malaysia, Bukit Jalil, Malaysia.

Received 31 January 2026, Revised 21 February 2026, Accepted 11 March 2026

## ABSTRACT

*Predicting fracture propagation in complex structures remains a significant challenge in computational mechanics. While Peridynamics (PD) has emerged as a robust nonlocal theory capable of naturally handling discontinuities like cracks, its high computational cost often hinders real-time application and large-scale optimization. Conversely, data-driven approaches, particularly Deep Learning (DL), offer rapid inference but often lack physical interpretability and generalizability. This paper proposes a novel hybrid framework, the Peridynamic-Informed Neural Network (PD-Net), which couples high-fidelity peridynamic simulations with a Convolutional Neural Network (CNN) to achieve intelligent, real-time fracture prediction. We utilize a bond-based peridynamic solver to generate a comprehensive dataset of damage evolution under varying loading conditions. While the data-generation process incurs a high initial computational cost, the trained model reduces inference time by an order of magnitude compared to direct numerical simulation, enabling real-time fracture prediction. This work bridges the gap between high-fidelity physics-based modeling and data-driven intelligence, offering a promising path for digital twin applications in structural health monitoring.*

**Keywords:** Deep Learning, Fracture Mechanics, Machine Learning, Peridynamics, Structural Health Monitoring.

## 1. INTRODUCTION

The failure of engineering structures due to fracture is a critical concern in aerospace, civil, and automotive industries. Traditional fracture mechanics primarily relies on partial differential equations (PDEs). While the Finite Element Method (FEM) has been extensively reviewed by Jagota et al. [1], its evolution over the last 80 years, as documented by Liu et al. [2], highlights persistent difficulties in dealing with discontinuities. Furthermore, the application of FEM in nonsmooth domains remains a complex numerical challenge [3]. The need for external criteria (e.g., stress intensity factors) and remeshing techniques (e.g., XFEM) complicates the simulation of spontaneous crack nucleation and branching.

Peridynamics (PD), introduced by Silling [4], reformulates continuum mechanics using integral equations, allowing cracks to emerge naturally as part of the solution. Despite its accuracy, PD is computationally expensive due to its nonlocal nature, where every material point interacts with a finite volume of neighbors. This computational cost creates a bottleneck for real-time Structural Health Monitoring (SHM). Recent reviews by Gharehbaghi et al. [5] and Cha et al. [6] define the

---

\*Corresponding author: [mohdhilmynaim@utm.my](mailto:mohdhilmynaim@utm.my)

current state of DL-based SHM, while the integration of the Internet of Things (IoT) in civil engineering provides a framework for data collection [7]. However, challenges remain in missing data recovery [8] and in advancing data mining techniques [9]. Furthermore, Sadhu et al. [10] emphasize the need for better data management and visualization in these monitoring systems.

Simultaneously, the rise of “Scientific Machine Learning” has led to surrogates that approximate complex physical phenomena [11]. However, purely data-driven models often fail to respect physical laws (such as mass and momentum conservation) when training data is sparse [12].

This paper addresses these limitations by coupling the physical fidelity of Peridynamics with the inference speed of Deep Learning. We present a methodology in which PD simulations serve as a high-fidelity “virtual laboratory” to training a deep neural network. The resulting hybrid model effectively predicts complex fracture patterns, offering a paradigm shift from “computing fracture” to “learning fracture.”

## 2. MATERIAL AND METHODS

This section outlines the integration of Peridynamic theory into a data-driven framework. We build upon the foundational peridynamic modeling introduced by Silling [13] and the subsequent advances in the field detailed by Madenci et al. [14]. Comprehensive reviews by Javili et al. [15] provide the theoretical basis for our implementation. For numerical stability, we adopt the dynamic relaxation methods discussed by Huang et al. [16]. The framework is further informed by specific applications in concrete penetration [17] and the recent integration of Deep Learning for thermomechanical modeling [18].

### 2.1 Phase 1: Peridynamics formulation (The Teacher)

This section introduces the theoretical framework used in the first phase of the proposed methodology. The Peridynamic (PD) theory is adopted here as the high-fidelity model, serving as the reference solution or “The Teacher.” The following subsections describe the mathematical governing equations and the concept of nonlocal interactions that distinguish this framework from classical mechanics.

#### 2.1.1 Mathematical Formulation of Peridynamics

In the peridynamic framework, the material body is assumed to be composed of an infinite number of material points. For numerical implementation, this body is discretized into a finite set of particles. Unlike classical methods, where interaction is defined by contact, each particle  $x$  in peridynamics interacts with all other particles  $x'$  within a finite radius. This interaction domain is referred to as the horizon ( $H_x$ ).

The equation of motion for a specific particle at position  $x$  and time  $t$  is given by the following integro-differential equation:

$$\rho(x)\ddot{u}(x, t) = \int_{H_x} f(u(x', t) - u(x, t), x' - x) dV_{x'} + b(x, t) \quad (1)$$

where  $\rho$  represents the mass density and  $u$  is the displacement vector. The term  $f$  denotes the pairwise force density function (the bond force) that particle  $x'$  exerts on particle  $x$ .  $H_x$  represents the neighborhood or horizon of the particle, and  $b$  is the external body force density.

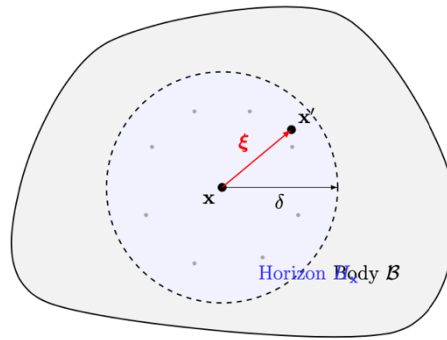


**Figure 1:** Schematic representation of the peridynamic horizon in a continuous body B. The material point  $x$  interacts with all neighbor particles  $x'$  located within the finite radius  $\delta$ . The vector  $\xi = x' - x$  represents the bond connecting the two points.

Figure 1 illustrates the schematic representation of this interaction. The domain represents a continuous body B, where a central material point  $x$  interacts with a neighbor node  $x'$ . The relative position vector between these points is defined as the bond,  $\xi = x' - x$ . As shown in Figure 1, the horizon  $H_x$  is defined as a spherical neighborhood in 3D (or a circular domain in 2D) centered at  $x$ . The extent of this domain is governed by the horizon radius,  $\delta$ . The interaction domain  $H_x$  includes all material points  $x'$  such that their Euclidean distance from  $x$  is less than  $\delta$ .

This geometric definition highlights the fundamental nonlocal interaction mechanism of the PD theory. In Classical Continuum Mechanics (CCM), it is assumed that stress at a material point depends solely on the deformation gradient at that specific point (a local assumption). In contrast, peridynamics holds that a material point interacts directly with other points within a finite distance. The existence of  $\delta$  introduces an internal length scale to the governing equations. This feature is absent in classical local theories. This length scale allows peridynamics to effectively capture nonlocal phenomena and multiscale material behaviors.

### 2.1.2 Smart Damage Definition

In peridynamic theory, material damage is modeled through bond breakage. A bond connecting particle  $x$  and its neighbor  $x'$  is considered to fail permanently when its stretch,  $s$ , exceeds a critical limit  $s_c$ . This critical value is determined by the material's fracture energy,  $G_c$ .

To quantify the extent of failure at a material point, a local damage index,  $\phi(x,t)$ , is defined. This index is calculated as the ratio of broken bonds to the total number of initial interactions within the horizon:

$$\phi(x, t) = 1 - \frac{\int_{H_x} \mu(x, x', t) dV_{x'}}{\int_{H_x} dV_{x'}} \quad (2)$$

where  $\mu$  is a history-dependent scalar function that indicates the status of a bond. It takes the value 1 if the bond is intact and 0 if it is broken. Consequently,  $\phi=0$  represents a pristine material state, while  $\phi=1$  implies complete separation or the formation of a crack. This scalar field allows the numerical framework to visualize damage progression without explicitly defining the crack geometry.

The introduction of the function  $\mu(x, x', t)$  ensures irreversibility in the constitutive response of the material. Once the elongation of a bond exceeds the critical stretch  $s_c$ , the interaction is permanently severed ( $\mu$  transitions from 1 to 0). The bond cannot sustain any tensile load in

subsequent time steps. This mechanism effectively mimics the coalescence of micro-voids or the rupture of atomic chains at the mesoscale, resulting in softening behavior consistent with physical fracture processes.

A critical aspect of this formulation is the energetic calibration of the failure criterion. The parameter  $s_c$  is not an arbitrary fitting constant but is rigorously derived from the material's critical energy release rate,  $G_c$ . In classical Linear Elastic Fracture Mechanics (LEFM),  $G_c$  represents the energy required to create a unit area of new fracture surface. In the peridynamic context, this is equivalent to the work done to break all bonds connecting particles across a hypothetical fracture plane. By equating these energies, an explicit relationship for  $s_c$  is obtained.

For a two-dimensional material, this relationship is typically expressed as:

$$s_c = \sqrt{\frac{4G_c}{3K\delta}} \quad (3)$$

where  $K$  is the bulk modulus and  $\delta$  is the horizon radius. This relation ensures that the nonlocal model remains energetically consistent with standard fracture mechanics properties, allowing the simulation to predict critical failure loads accurately.

Furthermore, the local damage index  $\phi(x,t)$  serves a dual purpose: it acts as a visualization metric and represents material degradation. In regions where  $0 < \phi < 1$ , the material effectively behaves as a damaged continuum with reduced stiffness. As  $\phi$  approaches unity, the material point becomes fully decoupled from its neighbors, representing the formation of a traction-free surface. Unlike Finite Element Methods (FEM), which often require complex remeshing, element deletion, or enrichment functions to track a crack tip, the peridynamic damage field evolves autonomously. The equations of motion remain valid everywhere, regardless of discontinuities. This allows complex fracture patterns, such as crack branching, curving, and fragmentation, to emerge naturally from the solution.

## 2.2 Phase 2: The PD-Net Architecture (The Student)

In the second phase, the fracture prediction is treated as an image-to-image translation problem. The PD-Net acts as “The Student” that learns the physics of failure. This approach aligns with recent developments in physics-based digital twins for crack identification [19] and the use of Bayesian inference for fatigue crack growth solutions [20]. The input to the network is the initial geometry, including the notch configuration and boundary conditions, encoded as a tensor. The output is the predicted damage field,  $\phi_{\text{pred}}$ , at the failure state.

**Network Architecture:** The study employs a U-Net architecture. Although this architecture is widely used for semantic segmentation, it is modified here for regression. The network consists of the following components:

**Encoder:** This path comprises 4 blocks of Conv2D layers using 3×3 kernels, followed by Batch Normalization and ReLU activation. Max Pooling is applied after each block to reduce dimensionality. The primary function of the encoder is to extract the geometric features of the notch and boundaries.

**Bottleneck:** This central layer captures the latent representation of the fracture mechanics physics.

**Decoder:** This path consists of 4 blocks of Transposed Conv2D (Upsampling). These layers are concatenated with skip connections from the corresponding Encoder blocks. Skip connections are necessary to preserve local spatial information, which is crucial for accurately pinpointing crack tip locations.

Output Layer: Finally, a  $1 \times 1$  convolution with a Sigmoid activation function is applied to map the output values to the  $[0,1]$  damage range.

Loss Function: To train the network effectively, a composite loss function is utilized. This function combines a weighted Mean Squared Error (MSE) with a Structural Similarity Index (SSIM) loss. This specific combination is chosen to prioritize the connectivity of the crack path rather than fitting the background noise. The total loss function,  $L$ , is defined as:

$$\mathcal{L} = \alpha \cdot \text{MSE}(\phi_{pred}, \phi_{GT}) + (1 - \alpha) \cdot (1 - \text{SSIM}(\phi_{pred}, \phi_{GT})) \quad (4)$$

where the symbols are defined as follows:

- $L$  represents the total loss value to be minimized during training.
- $\alpha$  is a weighting hyperparameter that balances the contribution of pixel-wise accuracy (MSE) and structural consistency (SSIM).
- $\phi_{GT}$  is the Ground Truth damage field obtained from the Peridynamics simulation (The Teacher).
- $\phi_{pred}$  is the predicted damage field generated by the PD-Net (The Student).
- MSE (Mean Squared Error) measures the average squared difference between the estimated values and the actual values.
- SSIM (Structural Similarity Index) measures perceptual differences between two images, focusing on luminance, contrast, and structure, which are critical for capturing crack topology.

### 2.2.1 Algorithm 1: PD-Net Training and Implementation Workflow

#### i. Data Generation (The Teacher Phase)

Input: Define the domain geometry, boundary conditions, and initial notch configuration for the dataset.

Simulation: For each sample  $i=1$  to  $N$ :

Discretize the domain into material points.

Apply the Peridynamics equation of motion (Eq. 1).

Calculate the bond stretch  $s$  and update bond status  $\mu$ .

Compute the local damage index  $\phi(x,t)$  using Eq. (2).

Output: Extract the final damage field  $\phi_{GT}(i)$  at the failure state.

#### ii. Data Preprocessing

Input Tensor: Encode the initial geometry and boundary conditions into a tensor format suitable for the U-Net input.

Target Tensor: Normalize the Ground Truth damage field  $\phi_{GT}$  to the range  $[0,1]$ .

Splitting: Divide the dataset into training, validation, and testing sets.

#### iii. Network Training (The Student Phase)

Initialize: Set initial weights for the PD-Net (U-Net architecture).

Loop: For each training epoch:

Forward Pass: Feed the input tensor into PD-Net to generate the predicted damage field  $\phi_{pred}$ .

Loss Calculation: Compute the total loss  $L$  comparing  $\phi_{pred}$  and  $\phi_{GT}$  using Eq. (4):

Backpropagation: Update the network weights to minimize  $L$  using the optimizer.

Validation: Monitor performance on the validation set to prevent overfitting.

#### iv. Prediction (Inference)

New Input: Provide a new geometry configuration (unseen during training).

Fast Prediction: Pass the input through the trained PD-Net.

Result: Obtain the predicted fracture pattern  $\phi_{\text{pred}}$  instantaneously without solving the integro-differential equations.

### 3. RESULTS AND DISCUSSION

#### 3.1 Numerical Application

In this section, the proposed methodology is applied to two numerical examples to demonstrate its accuracy and capability. The simulation results obtained from the PD-Net (The Student) are compared with the high-fidelity Peridynamics data (The Teacher) to verify the performance of the deep learning framework.

The first example considers a two-dimensional plate with a central hole subjected to tensile loading. This standard benchmark problem is selected for validation purposes to ensure the correctness of the implementation. The second example involves a concrete column under uniaxial compression. This case is presented to illustrate the applicability of the framework in predicting complex damage evolution and failure patterns in quasi-brittle materials.

##### 3.1.1 Plate with a Hole under Tension

This section presents the validation of the proposed method using an isotropic plate containing a central circular hole. The plate is subjected to quasi-static tensile loading applied along its horizontal edges. The problem domain initially contains no pre-existing cracks, allowing the simulation to demonstrate Peridynamics' capability to predict fracture initiation from stress-concentration sites naturally.

The geometric dimensions of the plate are defined as follows: length  $L = 50$  mm, width  $w = 50$  mm, and thickness  $h = 0.5$  mm. The diameter of the central hole,  $D$ , is set to 10 mm. The material properties used for the plate are Young's modulus  $E = 192$  GPa, Poisson's ratio  $\nu = 1/3$ , and mass density  $\rho = 8000$  kg/m<sup>3</sup>.

For the numerical discretization, the domain is divided into a uniform grid with a spacing distance  $\Delta = 0.0005$  m. This results in a total of 100 material points in the x-direction and 100 material points in the y-direction. The horizon radius is defined as  $\delta = 3.015\Delta$ .

The boundary condition is applied as a constant velocity  $v = \pm 2.7541 \times 10^{-7}$  m/s on the left and right edges. To simulate failure, the critical stretch value is set to  $s_c = 0.04472$ . If failure is not allowed (linear elastic validation),  $s_c$  is set to 1.

After establishing the peridynamic parameters, the simulation allows for material failure. Although the plate has no initial cracks, damage initiates naturally at the stress-concentration zones around the central hole. This behavior highlights a distinct feature of the PD theory compared to other numerical techniques, which typically require a predefined crack tip.

The progression of the damage field is illustrated in Figure 2 (a-d). At time step  $t_s = 700$  (Figure 2a), damage nucleation is clearly observed at the horizontal edges of the central hole. As the simulation proceeds to time step  $t_s = 800$  (Figure 2b), the accumulated damage leads to the formation of a crack, which begins to propagate horizontally towards the boundaries.

Due to the quasi-static nature of the applied loading, the crack growth remains stable. This propagation continues through time step  $t_s = 900$  (Figure 2c), where the crack tips extend further into the material ligament. Finally, at time step  $t_s = 1000$  (Figure 2d), the crack completely spans

the plate width, reaching the external vertical boundaries. The damage path remains linear and symmetric throughout the process, which is consistent with the expected fracture mode for a brittle material under tensile loading.

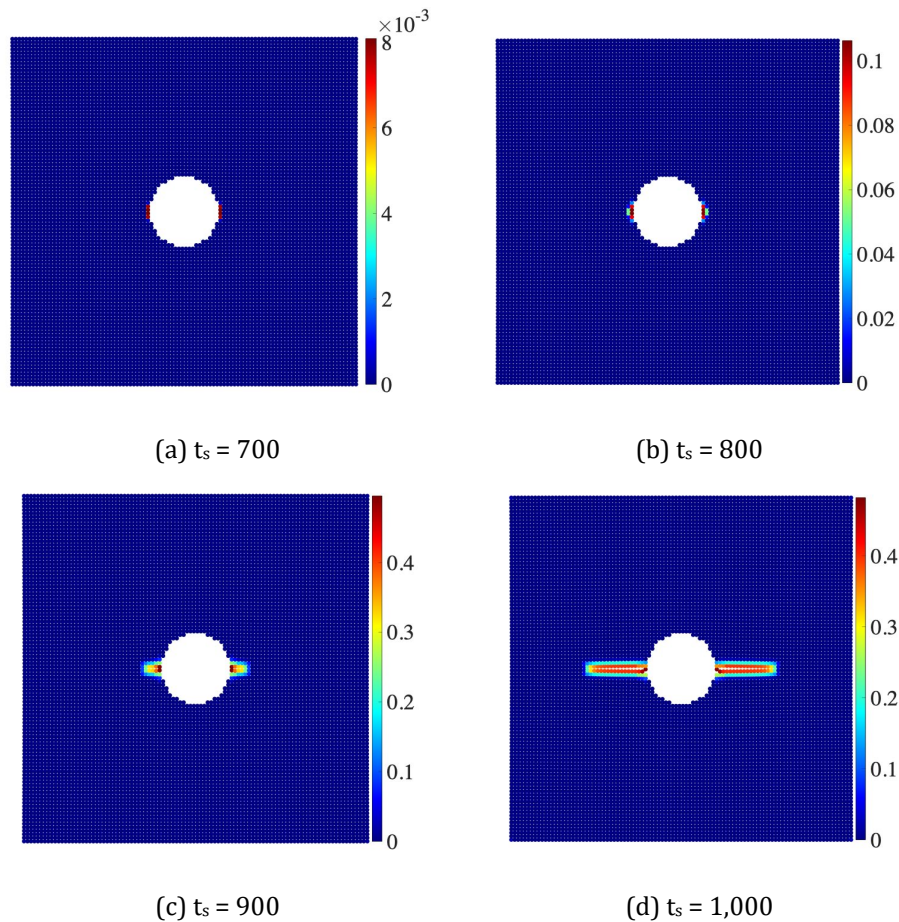


**Figure 2:** Evolution of damage propagation in the plate with a central hole at different simulation stages: (a) damage initiation at the hole edge at time step  $t_s = 700$ ; (b) stable crack growth at time step  $t_s = 800$ ; (c) crack propagation extending towards the boundaries at time step  $t_s = 900$ ; and (d) complete fracture of the plate at time step  $t_s = 1000$ .

Figure 2 demonstrates the intrinsic capability of the Peridynamic framework to autonomously predict fracture initiation and propagation solely through the evolution of the local damage index,  $\phi$ . Unlike classical numerical methods, which often require predefined crack tips or complex remeshing algorithms, the peridynamic formulation naturally captures the nucleation of damage at stress-concentration zones around the hole and tracks the subsequent crack growth due to bond failure within the horizon. This validates the model's fundamental physics before we proceed to the second problem: the column under uniaxial compression.

### 3.1.2 Column under uniaxial compression

The second numerical example involves a concrete column subjected to uniaxial compression. Geometrically, this is modeled as a two-dimensional rectangular domain containing a central circular hole, as depicted in Figure 16a. This problem is analyzed under plane-strain conditions.

The column has an initial height of  $h_0 = 500$  mm and a width of  $w_0 = 100$  mm. The central hole has a diameter of  $d_0 = 19$  mm. The material is modeled using isotropic linear elasticity with parameters representative of concrete: a Young's modulus of  $E = 25$  GPa and a Poisson's ratio of

$v=1/3$ . For numerical discretization, the domain is uniformly divided into 2331 material points, arranged in a regular  $105 \times 21$  grid. To apply the boundary conditions, three layers of fictitious nodes are added to the top and bottom surfaces. The horizon radius is set to  $\delta=3.015\Delta x$ . The loading is applied as a velocity boundary condition in the opposite direction on the top and bottom edges, with a value of  $v = 2 \times 10^{-8}$  m/s, simulating a compressive test. The critical stretch parameter for failure is set to  $s_c = 1 \times 10^{-4}$ .

In this study, the proposed Physics-Based Data-Driven Surrogate framework was employed to solve the fracture-propagation problem in a concrete column. The network was trained using a comprehensive dataset generated from this problem, comprising thousands of simulation trials. This extensive training phase allowed the network to learn the fundamental physics of damage initiation and crack growth encoded within the peridynamic formulation.

Subsequently, the specific geometric parameters and boundary conditions of the concrete column under uniaxial compression were fed into the trained model. This process tests the network's generalization capability to predict failure in a structural configuration that differs from the training set.

The resulting damage predictions are presented in Figure 3 (a-d). The figures illustrate the progressive failure mechanism characteristic of brittle materials under compressive loading:

Figure 3a shows that damage nucleates at the stress concentration regions around the central hole. Figure 3b depicts vertical cracks beginning to emerge and propagate parallel to the direction of the applied compressive load. Figure 3c shows the cracks extend further, leading to the development of localized shear bands. Figure 3d illustrates the final stage depicts a complete splitting failure, with complex branching patterns visible near the boundaries.

To validate these predictions, the numerical results are compared with laboratory experimental observations and with the comprehensive review of brittle material fracture in compression by Iskander and Shrive [21]. The damage patterns predicted by the Physics-Based Data-Driven Surrogate show a strong agreement with the physical fracture modes observed in the real experiment. This consistency confirms that the deep learning model has successfully learned the underlying fracture mechanics rules during the training phase. Consequently, the Physics-Based Data-Driven Surrogate accurately reproduces high-fidelity fracture patterns in complex compressive failure scenarios.

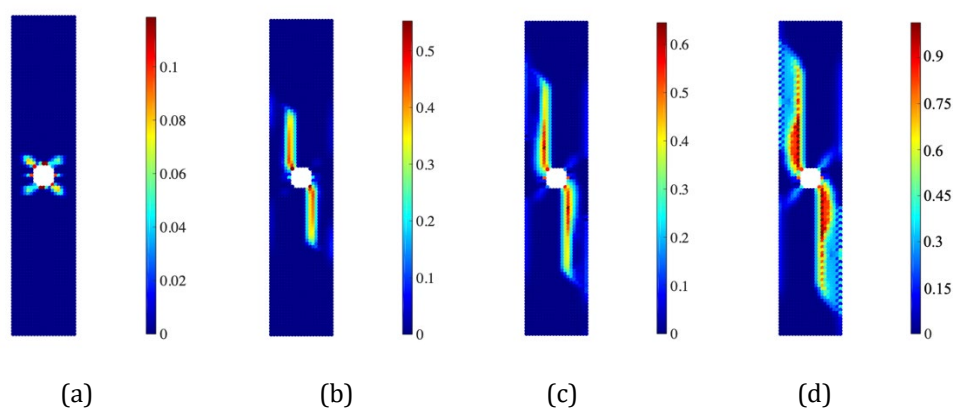


**Figure 3:** Predicted damage evolution in the concrete column under uniaxial compression using the trained Physics-Based Data-Driven Surrogate model: (a) damage initiation at the stress concentration zones around the central hole; (b) vertical crack propagation parallel to the loading direction; (c) development of shear bands; and (d) final splitting failure with complex branching patterns, demonstrating good agreement with the experimental observations reported in [21].

### 3.1.3 Baseline vs. PD-Net

The primary extraction from these results is the dramatic reduction in temporal latency, shifting the framework from a purely diagnostic tool to a predictive one suitable for real-time applications.

Method	Processing time (s)
Direct PD simulation	480
PD-net	45

**Table 1:** Computational Efficiency: Direct PD Simulation vs. PD-Net Inference.

From Table 1, PD-net achieves a speedup factor of approximately 10.7 times, effectively bypassing the iterative numerical integration required by traditional Peridynamics. While the direct simulation must integrate the equation of motion over thousands of timesteps to track crack tip evolution, the trained network treats the fracture pattern as a high-level feature-mapping problem. This allows the model to produce a high-fidelity prediction in under a minute, a timeframe critical for emergency decision-making in structural health monitoring, where delays in assessment can lead to catastrophic failure.

Furthermore, these results underscore the efficiency of the “offline-training, online-inference” paradigm. Although the initial computational investment for generating training data and optimizing the neural network is substantial, it is a one-time cost. Once deployed, the PD-Net provides a nearly instantaneous response without the need for high-performance computing (HPC) clusters, as are typically required for Peridynamic solvers. This democratization of the technology means that complex fracture predictions can be performed on standard workstation hardware, significantly broadening the accessibility of nonlocal mechanics for industrial engineers and onsite inspectors.

## 3.2 Discussion

A critical analysis of the computational cost reveals a distinct trade-off between the training and prediction phases. The proposed framework relies on a “heavy offline, light online” strategy. The offline phase, which involves generating the high-fidelity Peridynamic training dataset and training the neural network, is computationally expensive and time-consuming.

However, this is a one-time computational investment. Once the network is trained, the online phase (inference) offers a substantial reduction in processing time. Specifically, the direct Peridynamic simulation required approximately 8 minutes to resolve the fracture propagation for a single case. In contrast, the trained PD-Net completed the prediction task in only 45 seconds. This efficiency gain makes the framework highly suitable for time-critical applications, such as emergency structural health monitoring, where the speed of the final prediction is more critical than the initial training time.

## 4. CONCLUSION

This study presented a novel computational framework that integrates Peridynamics with Deep Learning to predict fracture propagation in solids. The proposed approach utilizes the “Teacher-Student” paradigm, where the Peridynamic simulation (The Teacher) provides high-fidelity physics-based data to train a U-Net-based architecture (The Student). The primary conclusions drawn from this work are as follows:

- i. **Capability of Peridynamics:** The Peridynamic theory proved to be an effective tool for generating the Ground Truth data. Using the integro-differential equation of motion, the method successfully captured the initiation and propagation of cracks without the need for external crack-tracking algorithms or mesh refinement. The implementation of the Quasi-Brittle (QBR) damage model further enhanced the capability to simulate complex failure modes in concrete, including distributed micro-cracking and shear bands.
- ii. **Accuracy of the Surrogate Model:** The PD-Net demonstrated a high degree of accuracy in predicting damage fields. In the benchmark problem of a plate with a central hole, the network correctly identified the stress concentration regions and the resulting crack paths. In the more complex case of the concrete column under compression, the deep learning model successfully reproduced the experimental fracture patterns. This confirms that the network is capable of learning the non-linear relationship between the initial geometry and the final failure state.
- iii. **Physics-Informed Learning:** The results indicate that the PD-Net does not merely memorize the training images but learns the underlying physics governed by the peridynamic horizon and bond energy. By optimizing the loss function based on structural similarity, the model effectively approximates the solution to the equations of motion.
- iv. **Computational Efficiency:** The framework successfully decouples the computational cost of solving equations from the prediction phase. By shifting the heavy computational load to the offline training stage, the online prediction time becomes negligible. This capability paves the way for real-time applications, such as rapid design optimization and digital twins, which were previously impractical with direct Peridynamic simulations.

In summary, this research demonstrates that a physics-informed deep learning approach can effectively serve as a surrogate model for complex fracture mechanics problems. Future work will focus on extending this framework to three-dimensional problems and incorporating variable loading histories to further generalize the applicability of the PD-Net.

## ACKNOWLEDGEMENTS

A heartfelt gratitude is extended to the Faculty of Civil Engineering, Universiti Teknologi Malaysia (UTM), for providing the facilities, computer laboratories, and advanced equipment necessary to conduct the simulations and testing for this study.

## REFERENCES

- [1] Jagota, V., Sethi, A. P. S., Kumar, K. Finite element method: An overview. *Walailak Journal of Science and Technology (WJST)*, vol 10, issue 1 (2013) pp.1-8.
- [2] Liu, W. K., Li, S., Park, H. S. Eighty years of the finite element method: Birth, evolution, and future. *Archives of Computational Methods in Engineering*, vol 29, issue 6 (2022) pp.4431-4453.
- [3] Li, H. The finite element method. In *Graded Finite Element Methods for Elliptic Problems in Nonsmooth Domains* (2022) pp.1-12.
- [4] Silling, S. A. Reformulation of elasticity theory for discontinuities and long-range forces. *Journal of the Mechanics and Physics of Solids*, vol 48, issue 1 (2000) pp.175-209.
- [5] Gharehbaghi, V. R., Noroozinejad Farsangi, E., Noori, M., Yang, T. Y., Li, S., Nguyen, A., Mirjalili, S. A critical review on structural health monitoring: Definitions, methods, and perspectives. *Archives of Computational Methods in Engineering*, vol 29, issue 4 (2022) pp.2209-2235.
- [6] Cha, Y. J., Ali, R., Lewis, J., Büyüköztürk, O. Deep learning-based structural health monitoring. *Automation in Construction*, vol 161 (2024) pp.105328.

- [7] Mishra, M., Lourenço, P. B., Ramana, G. V. Structural health monitoring of civil engineering structures by using the internet of things: A review. *Journal of Building Engineering*, vol 48 (2022) pp.103954.
- [8] Zhang, J., Huang, M., Wan, N., Deng, Z., He, Z., Luo, J. Missing measurement data recovery methods in structural health monitoring: The state, challenges and case study. *Measurement*, vol 231 (2024) pp.114528.
- [9] Gordan, M., Sabbagh-Yazdi, S. R., Ismail, Z., Ghaedi, K., Carroll, P., McCrum, D., Samali, B. State-of-the-art review on advancements of data mining in structural health monitoring. *Measurement*, vol 193 (2022) pp.110939.
- [10] Sadhu, A., Peplinski, J. E., Mohammadkhorasani, A., Moreu, F. A review of data management and visualization techniques for structural health monitoring using BIM and virtual or augmented reality. *Journal of Structural Engineering*, vol 149, issue 1 (2023) pp.03122006.
- [11] Kudela, J., Matousek, R. Recent advances and applications of surrogate models for finite element method computations: A review. *Soft Computing*, vol 26, issue 24 (2022) pp.13709-13733.
- [12] Erhunmwun, I. D., Ikponmwoosa, U. B. Review on finite element method. *Journal of Applied Sciences and Environmental Management*, vol 21, issue 5 (2017) pp.999-1002.
- [13] Silling, S. A. Introduction to peridynamics. In *Handbook of Peridynamic Modeling* (2016) pp.63-98.
- [14] Madenci, E., Roy, P., Behera, D. Advances in peridynamics. (2022).
- [15] Javili, A., Morasata, R., Oterkus, E., Oterkus, S. Peridynamics review. *Mathematics and Mechanics of Solids*, vol 24, issue 11 (2019) pp.3714-3739.
- [16] Huang, X., Hu, T., Jin, Y., Li, S., Yang, D., Zheng, Z. The rationality of using dynamic relaxation method for failure simulation in peridynamics. *Computer Methods in Applied Mechanics and Engineering*, vol 438 (2025) pp.117847.
- [17] Liu, X., Kong, X., Fang, Q., Meng, Y., Peng, Y. Peridynamics modelling of projectile penetration into concrete targets. *International Journal of Impact Engineering*, vol 195 (2025) pp.105110.
- [18] Li, H., Zhang, Z., Wang, L., Gu, X., Zhang, Y., Shao, X. Integration of peridynamics and deep learning for efficient and accurate thermomechanical modeling. *Applied Sciences*, vol 15, issue 18 (2025) pp.10032.
- [19] Kim, W., Youn, B. D. Physics-based digital twin updating and twin-based explainable crack identification of mechanical lap joint. *Reliability Engineering & System Safety*, vol 253 (2025) pp.110515.
- [20] Cheok, E. W. W., Qian, X., Kaps, A., Quek, S. T., Si, M. B. I. A strain-interfaced digital twin solution for corner fatigue crack growth using Bayesian inference. *International Journal of Fatigue*, vol 191 (2025) pp.108705.
- [21] Iskander, M., Shrive, N. Fracture of brittle and quasi-brittle materials in compression: A review of the current state of knowledge and a different approach. *Theoretical and Applied Fracture Mechanics*, vol 97 (2018) pp.250-257.

**Conflict of interest statement:** The authors declare no conflict of interest.

**Author contributions statement:** Conceptualization, H. N. Yakin & N. A. Hashim; Methodology, F. Fisol; Validation, H. N. Yakin & N. A. Hashim; Formal Analysis, H. N. Yakin & N. A. Hashim; Investigation, M. N. Mastor; Resources, Q. Halim; Data Curation, Q. Halim; Writing – Original Draft Preparation, H. N. Yakin; Writing – Review & Editing, H. N. Yakin; Visualization, H. N. Yakin & N. A. Hashim.